Simulation and exergoeconomic analysis of the syngas and biodiesel production process from spent coffee grounds

Diana L. Tinoco-Caicedo [a,b,c,*], Medelyne Mero-Benavides [a], Myrian Santos-Torres [a], Alexis Lozano-Medina [c], Ana M. Blanco-Marigorta [c]

[a] Facultad de Ciencias Naturales y Matemáticas (FCNM), Escuela Superior Politécnica del Litoral Ecuador, 090903, Guayaquil, Ecuador
[b] Centro de Energías Renovables y Alternativas (CERA), Escuela Superior Politécnica del Litoral Ecuador, 090903, Guayaquil, Ecuador
[c] Department of Process Engineering, Universidad de Las Palmas de Gran Canaria, 35017, Las Palmas de Gran Canaria, Canary Islands, Spain

A R T I C L E   I N F O

A B S T R A C T

The integrated production of biofuels from agro-industrial wastes is increasing around the world. The thermodynamic performance and economic analysis of these processes have become topics of interest given the need to reduce the cost of biofuels and their impact on the environment. This study develops a simulation of the production process of syngas and biodiesel from spent coffee grounds, and an exergoeconomic analysis that mainly determines the exergy destruction rate, the investment and operational cost rate, and the exergy destruction cost rate at component level and for the overall system. The total investment cost for the integrated process resulted in 13.2 million dollars. The specific cost of syngas and biodiesel from spent coffee grounds were estimated in $0.36/kg and $0.71/kg, respectively. The results show that the drying process including the air heating for the pretreatment of the biomass had an exergy destruction rate of 11,463 kW and was responsible of the 92% of the overall exergy destruction cost rate. An increment of the dead state temperature reduced the specific cost of syngas and biodiesel in 17% and 8%, respectively. Future studies should focus on the exergoeconomic optimization of the drying process of biomass in order to minimize the operational costs.

1. Introduction

Currently, fossil fuels are the primary source of energy. Approximately, 80% of the word's energy demand is supplied by them [1]. However, it's estimated that oil reserves would not be sufficient to meet the demand by 2050 [2]. To overcome this problem, it's important to look for renewable energy sources, especially in sectors that consume more energy: industries and transport [3]. Biofuels are one of the most common renewable energy sources and are considered the best option for industries especially when biofuel comes from an industrial waste [4]. During 2018, according to British Petroleum company, the United States became the first country with an annual production of 38.1 million tons of biofuel, followed by Brazil with a production of 21.4 million tons per year [5]. Nowadays there are 803 biorefineries in Europe where 45% of them produce biofuels [6]. The biofuels mostly produced are biodiesel, syngas and bioethanol [7]. In the last few years, different countries have produced biofuels from different sources, such as waste deriving from agriculture [8], agroindustry [9] and livestock [10]. These have gradually contributed to the reduction of 80% of the greenhouse

emissions from landfills [11].

The agricultural wastes that have been studied to be converted to biofuels included rice bran [12], oat straw [13], fish waste [14], alga [15] and spent coffee grounds (SCG) [16], where the last one has the highest calorific value (22 MJ/kg) and oil content (29%), becoming one of the best energetic potential resources for the production of liquid and solid biofuels. There are many experimental studies about the production of biofuels from SCG at laboratory scale. Liu et al. [17] studied the biodiesel production by applying in-situ transesterification method at 70 °C by 3 h, obtaining a yield of 98,61% greater than the 83% obtained by Haas et al. [18]. Meanwhile, Park et al. [19] applied indirect transesterification to the humidified SCG for the production of biodiesel and obtained a yield of 16.75%. Pacioni et al. [20] applied the gasification process with steam in a tubular reactor to produce syngas from SGC with a yield of 88.6%. Kibret et al. [21] applied the same process by using a semi-fluized bed and increased the yield to 95%.

In the last few years, many exergetic and exergoeconomic analyses of different biodiesel and syngas production processes have been developed in order to evaluate the sustainability of these processes. In the case of biodiesel, Antonova et al. [22] evaluated the production of biodiesel from the oil of canola seeds and found that the dryer and the transesterification reactor destroyed 7.8% and 25.2% of the fuel exergy rate, respectively. Amelio et al. [23] shows that an exergetic optimization in the biodiesel production from triolein oil achieves a higher reduction than energetic optimization, with a difference of 44.7 kW. Mancebo et al. [24] achieved an increase in the exergetic efficiency through an exergetic optimization from 10% to 22% and the reduction of exergy destruction cost rate from $0.13/h to $0.12/h. In the case of syngas, Shayan et al. [25] analyzed the gasification process of wood and determined the optimum temperature of gasification which allowed them to increase the exergetic efficiency by 24.9% and reduce the exergy destruction cost rates by 8.9%. Another similar study determined that the exergetic efficiency could be increased to 76.2% when the steam/biomass mass ratio is 1.83 [26]. Different exergetic analysis have been performed in processes that include a gasifier in combination with other treatments such as hydrotreatment, hydrocracking, steam reforming [27], direct and indirect synthesis of dimethyl ether [28], digestion plants [29] and integrated energy system [30]. In all these processes, the component with the highest exergy destruction rate was the gasifier.

As it is shown, although there are many experimental analysis on SCG that have demonstrated a high potential to be converted to biofuels, there are not exergetic and economic analyses focused on evaluating the sustainability of this process. The previous exergoeconomic analysis mentioned were only focused on evaluating specific steps such as transesterification or gasification of other types of biomass. Therefore, an exergetic and economic analyses of an integrated process for the production of biodiesel and syngas by indirect transesterification and gasification from SCG has never been reported.

In an effort to address the gap found in the literature, the aim of this study is to perform an exergetic and exergoeconomic analyses of an integrated production process of biodiesel and syngas from SCG. The process is simulated and validated with experimental data from previous studies. It includes drying of biomass, oil extraction, gasification of biomass, and indirect transesterification of the oil. The analyses allow us to identify the main components that have the highest exergy destruction rates and exergetic cost rates. The findings obtained herein can be useful for the design and optimization of biorefineries based on SCG.
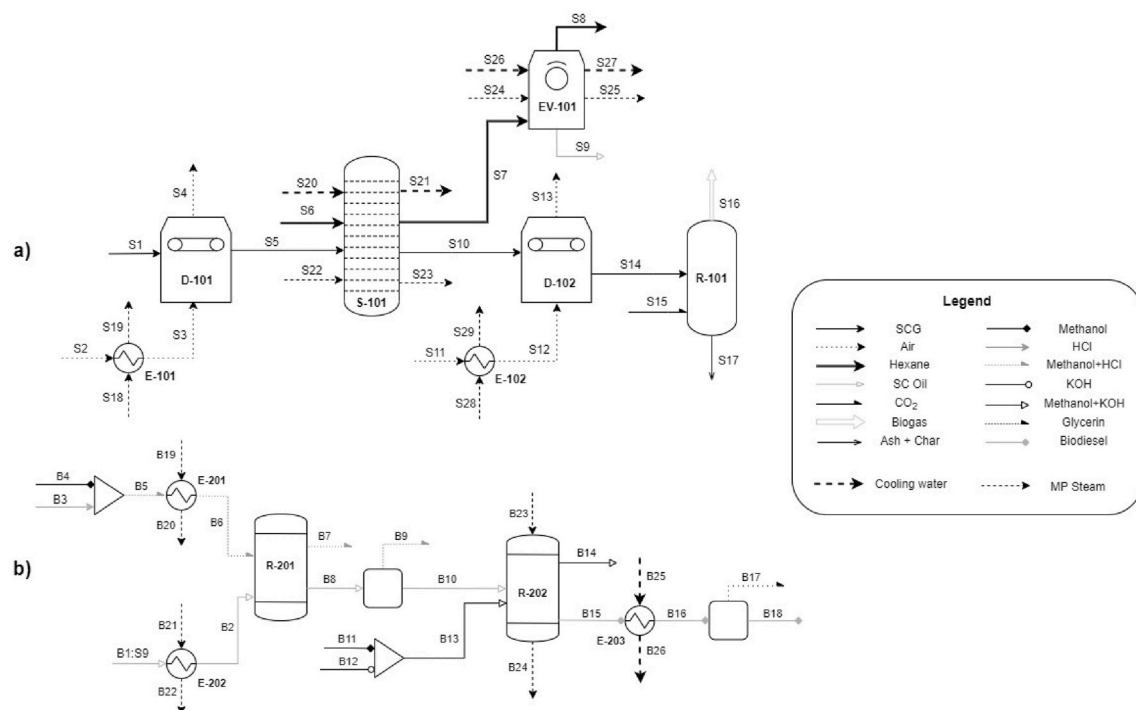

Fig. 1. Process flow diagram of the integrated process to produce a) syngas and b) biodiesel.

2. Materials and methods

2.1. System description

Fig. 1 shows the production of syngas and biodiesel from SCG with initial moisture of 61.1% w/w. Air (stream S3) is heated up to 150 °C (stream S4) in a heat exchanger (E−101), then it enters a dryer (D-101) to reduce the SCG's moisture to 12.4% w/w. The dried biomass (Stream S5) enters the soxhlet extractor (S-101), where it is in contact with hexane (stream S6) to extract 15% of the lipids from the SCG. The oil stream enters into a flash evaporator (EV-101) to recover the hexane (stream S8) and separate it from the lipids (stream S9). Traces of solvent in the spent biomass are evaporated in the dryer (D-102) with air preheated to 100 °C (stream S12). Then, the dried SCG enters a gasifier at 900 °C with carbon dioxide as the gasifying agent (stream S15) and produces syngas (stream 16), with a relative molar composition of 0.02, 0.43, 0.10, 0.37 for H_2, CH_4, CO, and CO_2, respectively [31]. In addition, the gasifier produces a solid stream with 95% char and 5% ash (stream 17). SCG oil (stream S9) is heated in a heat exchanger (E−202) with steam (stream B21) to 54 °C (stream B6). A mixture of methanol (stream B4) and hydrogen chloride (stream B3) is heated in a heat exchanger (E−201) with steam (stream B19) up to 54 °C. The heated mixture enters into a reactor (R-201) where the esterification reaction occurs to obtain methyl esters from free fatty acids. The methyl esters and the triglycerides of the oils leave the reactor (steam B8). Other products like excess reagent and produced water leave the reactor separately (stream B7). The product is decanted before going into the second reactor to eliminate the residues of methanol, water and HCl. In the second transesterification reactor (R-202), triglycerides from SCG oil (stream B10) react with methanol and KOH (stream B12) to produce water as a by-product (stream B14) and a mixture of glycerin and biodiesel as a product (stream B15). The product from the second reactor is cooled to room temperature (stream B16) and decanted to separate the glycerin (stream B17) from the biodiesel (stream B18).

2.2. Process simulation

The simulation of the process was performed in Aspen Plus V12.1. The SCG and the ash were simulated as unconventional components. Proximate and ultimate analyses were defined by applying the enthalpy and density model of the unconventional components (HCOALGEN and DCOALIGT) [32]. The oil chemical composition extracted from the SCG was obtained from a previous study [33], therefore the chemical compounds were simulated as conventional components using the NIST ThermoData Engine (TDE) database [34].

The conditions of the D-101 such as air/SCG mass ratio and initial and final humidity were established from experimental data in a convective dryer [35]. The EV-101 was simulated as a flash separator and a total solvent recovery was assumed. The ideal thermodynamic model was used for the gasification process because the pseudo-components were at a low pressure of 101.3 kPa [36]. The gasifier was simulated by the use of the RYIELD and the RGIBBS reactors [37]. Tar formation was not considered [38] and char was defined as pure coal, which was determined by the mass of fixed coal in the biomass.

For the esterification and transesterification processes, the UNIQUAC thermodynamic model was used, because the studied system has two liquid phases, some strong polar compounds and is at a low pressure of 101.3 kPa [39]. A yield of 100% and 85% were considered for the esterification and transesterification reactions occurring in R-201 and R-202, respectively, according to previous studies [40].

2.3. Model validation

The final moisture obtained in the dryers, the syngas composition obtained in the gasifier, the yield achieved in the oil extraction process, and the yield and composition of the biodiesel produced in the transesterification reactor were compared with the results obtained experimentally by previous studies using the same operational conditions, to ensure the validity of the modeled processes. For the esterification and the transesterification reactors, the operating conditions of Haile et al. [40] were used. The esterification reactor was operated at atmospheric pressure, with a methanol/FFA molar ratio of 20:1 and HCl at 10% w/w free fatty acids. The transesterification reactor had a methanol/oil molar ratio of 9:1 and KOH and 1% w/w of oil content. The D-101 was operated with the conditions presented in the experimental study of Gómez et al. [35].

The drying air temperature was 150 °C, and its relative humidity was 50%. The SCG initial moisture was 61.1% w/w. The inlet air flow was 524.8 kg wet air per kg of wet biomass.

For the soxhlet extraction the solvent/biomass mass ratio was 9.87 as used by De Melo et al. [41]. The gasifier was operated at 900 °C, with a CO_2/SCG molar ratio of 0.17 and with initial biomass moisture of 2.89% w/w, which are the conditions proposed by Kibret et al. [21].

2.4. Exergetic analysis

The exergetic analysis was conducted at the level of each system component. The Engineering Equations Solver (EES) software was used for the calculations. The enthalpy and entropy of most of the states were determined with the thermophysical properties library of EES, when possible. The specific heat capacity expressions for substances were not included in the EES database, such as SCG [42], lipids [43], ash [44], char [45] and glycerin [46], they were found in the literature.

The physical exergy and chemical exergy of the material streams were calculated using Eq. (1) and Eq. (2), respectively.

$$e_i^{PH} = h_i - h_o - T_o(s_i - s_o) \tag{1}$$

$$e_i^{CH} = \sum x_i e_i^{ch} + RT_o \sum x_i \ln(x_i) \tag{2}$$

where $T_0 = 27\ ^{\circ}C$ is the temperature of the dead state (with a dead state pressure of 1 atm), which is the annual average temperature in Guayaquil, Ecuador. x_i and e_i^{ch} are the molar composition and the standard chemical exergy, respectively of each compound presented in the stream i. The standard chemical exergies were obtained from the Model II [47].

The chemical exergy of moist air was calculated with Eq. (3) [48].

$$e_{air}^{ch} = 0.2857 c_{p,air} T_o ln \left[\left[\frac{1 + 1.6078 w_o}{1 + 1.6078 w} \right]^{(1+1.6078w)} \left[\frac{w}{w_o} \right]^{1.6078w} \right] \tag{3}$$

The exergy of wet biomass was calculated by using Eq. (4) [49] where x_{DB} is the composition of SCG in a dry free ash basis.
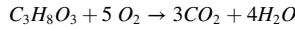
$$e_{WB}^{ch} = x_{DB} \cdot e_{DB}^{ch} + \sum x_i \cdot e_i^{ch} \tag{4}$$

The chemical exergy of the ashes was calculated by using the model proposed by Song et al. [50] which is based on a statistical study of ash in 86 varieties of biomass and depends on the total concentration of different minerals. For SCG, this total concentration was obtained from a study conducted on coffee waste [51]. The chemical exergies of SCG, defatted SCG, oil, char and the biodiesel were determined by using Eq. (5) applied to pure hydrocarbon fuels [49]. The molecular formula of each of these substances was estimated based on their respective ultimate analysis.

$$e_x^{ch} = \overline{HHV}(T_o, P_o) - T_o \left[\sum_R v_R \overline{s}_R - \sum_P v_P \overline{s}_P \right](T_o, P_o) - \left[\sum_P v_P \overline{e}_P^{ch} - \sum_R v_R \overline{e}_R^{ch} \right] \tag{5}$$

where $\overline{HHV}$ represents the higher heating value at the dead state conditions; v is the stochiometric coefficient of each combustion compound, and $\overline{s}$ the standard entropy of each compound. The higher heating values of SCG oil [40], biodiesel [52], SCG and defatted SCG [32], and char [20] were obtained from literature.

For the calculation of the chemical exergy of glycerin, a reaction involving reference substances has been considered:

$$C_3H_8O_3 + 5\ O_2 \rightarrow 3CO_2 + 4H_2O$$

Eq. (6) was used for the determination of the chemical exergy of glycerin [49]; where ΔG is the change in the Gibbs function at dead state conditions.

$$e_{gly}^{ch} = \Delta G - \left[\sum_P v_P \overline{e}_P^{ch} - \sum_r v_R \overline{e}_R^{ch} \right] \tag{6}$$

The exergy balance of each component of the process was performed according to Bejan et al. [49] using Eq. (7):

$$\dot{E}_{F,k} - \dot{E}_{P,k} = \dot{E}_{D,k} - \dot{E}_{L,k} \tag{7}$$

where $\dot{E}_{F,k}$ corresponds to the fuel exergy, $\dot{E}_{P,k}$ is the product exergy, $\dot{E}_{D,k}$ is the destroyed exergy and $\dot{E}_{L,k}$ is the exergy loss. Table 1

Table 1
Definitions of fuel and product exergy for each component.

Component	$\dot{E}_F$	$\dot{E}_P$
Heat exchanger (E−101)	$\dot{E}_{S18} - \dot{E}_{S19}$	$\dot{E}_{S3} - \dot{E}_{S2}$
Dryer (D-101)	$\dot{E}_{S1} + \dot{E}_{S3}$	$\dot{E}_{S5}$
Soxhlet extractor (S-101)	$(\dot{E}_{S22} - \dot{E}_{S23}) - (\dot{E}_{S21} - \dot{E}_{S20}) + (\dot{E}_{S5} - \dot{E}_{S10})$	$\dot{E}_{S7} - \dot{E}_{S6}$
Evaporator (EV-101)	$(\dot{E}_{S24} - \dot{E}_{S25}) + \dot{E}_{S7} - (\dot{E}_{S27} - \dot{E}_{S26})$	$\dot{E}_{S8} + \dot{E}_{S9}$
Heat exchanger (E−102)	$\dot{E}_{S28} - \dot{E}_{S29}$	$\dot{E}_{S12} - \dot{E}_{S11}$
Dryer (D-102)	$\dot{E}_{S10} + \dot{E}_{S12}$	$\dot{E}_{S14}$
Reactor (R-101)	$\dot{E}_{S14} + \dot{E}_{S15} - \dot{E}_{S17}$	$\dot{E}_{S16}$
Heat exchanger (E−201)	$\dot{E}_{S19} - \dot{E}_{S20}$	$\dot{E}_{B6} - \dot{E}_{B5}$
Heat exchanger (E−202)	$\dot{E}_{S21} - \dot{E}_{S22}$	$\dot{E}_{B2} - \dot{E}_{B1}$
Heat exchanger (E−203)	$\dot{E}_{B15} - \dot{E}_{B16}$	$\dot{E}_{B26} - \dot{E}_{B25}$
Reactor (R-201)	$\dot{E}_{B6} + \dot{E}_{B2} - \dot{E}_{B7} - \dot{E}_{B9}$	$\dot{E}_{B10}$
Reactor (R-202)	$(\dot{E}_{B13} - \dot{E}_{B14}) + (\dot{E}_{B23} - \dot{E}_{B24}) + \dot{E}_{B10}$	$\dot{E}_{B15}$
Overall system	$\dot{E}_{heating} - \dot{E}_{cooling} + \dot{E}_{S6} - \dot{E}_{S8} + \dot{E}_{S1} + \dot{E}_{S15} + \dot{E}_{B5} - (\dot{E}_{B7} - \dot{E}_{B9}) + \dot{E}_{B13} - \dot{E}_{B14}$	$\dot{E}_{B16} + \dot{E}_{S16}$

presents the definitions of the fuel and product exergy for each component of the process. For the overall system, the $\dot{E}_{heating}$ is the sum of the changes of exergy rates of the streams of steam used in the heating processes. $\dot{E}_{cooling}$ is the sum of the change of exergy rates of the streams of cooling water used in the cooling processes.

2.5. Economic analysis

The economic analysis was performed by following the Total Revenue Requirement methodology [49]. The purchase equipment cost (PEC) for each component of the process was obtained from vendors based on the required characteristics and are presented in the results section. The costs of steam and carbon dioxide were considered as $0.03/kg and $24.22/kg, respectively [53]. The cost of cooling water [54] is $0.72/m^3. The cost of n-hexane, methanol, hydrogen chloride and sodium hydroxide were $0.03/kg, $1.15/kg, $0.50/kg, $0.04/kg, respectively, which were obtained from vendors.

The total cost rate for operation and investment ($\dot{Z}_k$) was determined as is shown in Eq. (8).

$$\dot{Z}_k = \dot{Z}_k^{O\&M} + \dot{Z}_k^{CI} \tag{8}$$

where $\dot{Z}_k^{CI}$ is the capital investment cost rate and $\dot{Z}_k^{O\&M}$ is the operation and maintenance cost rate of the kth component. These variables were calculated by using the economic indicators presented in Table 2, obtained from a previous study [49].

2.6. Exergoeconomic analysis

The exergoeoconomic analysis was carried out by performing a cost balance in each component of the system following Eq. (9):

$$\dot{C}_{F,\,k} + \dot{Z}_k = \dot{C}_{P,\,k} \tag{9}$$

where $\dot{C}_{F,\,k}$ and $\dot{C}_{P,\,k}$ are the fuel and the product cost rate of the k-th component, respectively. These costs were determined following the expressions from Table 3. The exergoeconomic indicators such as the exergoeconomic factor (f_k), the relative cost difference (r_k), and the exergy destruction cost rate ($\dot{C}_D$) for each component of the system were calculated following the methodology reported by Bejan et al. [49].

3. Results and discussions

3.1. Model validation

In order to verify the validity of each component's calculation models, the values of the main operating parameters obtained in this work have been compared with those reported in experimental studies from other literature. On Table 4, the final moisture obtained in the dryer (D-101), the yield of the Soxhlet extractor (S-101), the syngas composition that is produced in the gasifier (R-101) and the yield and biodiesel composition produced in the reactor (R-202) were presented and compared. It can be observed that the results of the model are close to the results reported in the experimental studies, with a maximum absolute error of 5.3, which represents a 6% relative error. Therefore, it is concluded that the models can be used to represent the syngas and biodiesel production process from SCG oil under the established operating conditions.

3.2. Exergetic analysis

Table 5 shows the mass flow rate ($\dot{m}$), the temperature (T), the pressure (P), the specific enthalpy (h), the specific entropy (s), the physical exergy ($\dot{E}^{ph}$), the chemical exergy ($\dot{E}^{ch}$) and the total exergy ($\dot{E}$) of each material stream. It can be observed that the chemical exergy is higher than the physical exergy in most of the states, especially in the streams that have lipids, hexane, biomass, and its

Table 2
Economic parameters used for the economic analysis [49].

Parameter	Value
Average general inflation rate	0.05
Average nominal escalation of all costs	0.05
Average nominal escalation of fuel costs	0.05
Plant economic life in years (n)	20
Plant life for tax purposes in years	15
Average combined income tax rate	0.38
Average property tax rate (%PFI)	0.015
Average insurance rate (%PFI)	0.5
Average capacity factor	0.85
Labor positions for O&M	20
Average labor rate ($/h)	18

Table 3
Cost balance equations and auxiliary equations for exergy costs of the system.

Component	Fuel Cost	Product Cost	Auxiliary Equations
E−101	$\dot{C}_{S18} - \dot{C}_{S19}$	$\dot{C}_{S3} - \dot{C}_{S2}$	$c_{S2} = 0$ $c_{S19} = c_{S18}$
D-101	$\dot{C}_{S1} + \dot{C}_{S3}$	$\dot{C}_{S5}$	$c_{S1} = 0$
S-101	$(\dot{C}_{S22} - \dot{C}_{S23}) - (\dot{C}_{S21} - \dot{C}_{S20}) + (\dot{C}_{S5} - \dot{C}_{S10})$	$\dot{C}_{S7} - \dot{C}_{S6}$	$c_{S21} = c_{S20}$ $c_{S23} = c_{S22}$ $c_{S10} = c_{S7}$
EV-101	$(\dot{C}_{S24} - \dot{C}_{S25}) + \dot{C}_{S7} - (\dot{C}_{S27} - \dot{C}_{S26})$	$\dot{C}_{S8} + \dot{C}_{S9}$	$c_{S25} = c_{S24}$ $c_{S27} = c_{S26}$ $c_{S8} = c_{S9}$
E−102	$\dot{C}_{S28} - \dot{C}_{S29}$	$\dot{C}_{S12} - \dot{C}_{S11}$	$c_{S11} = 0$ $c_{S29} = c_{S28}$
D-102	$\dot{C}_{S10} + \dot{C}_{S12}$	$\dot{C}_{S14}$	–
R-101	$\dot{C}_{S14} + \dot{C}_{S15} - \dot{C}_{S17}$	$\dot{C}_{S16}$	$c_{S17} = c_{S16}$
E−201	$\dot{C}_{B19} - \dot{C}_{B20}$	$\dot{C}_{B6} - \dot{C}_{B5}$	$c_{B19} = c_{B20}$
E−202	$\dot{C}_{B21} - \dot{C}_{B22}$	$\dot{C}_{B2} - \dot{C}_{B1}$	$c_{B21} = c_{B22}$
E−203	$\dot{C}_{B15} - \dot{C}_{B16}$	$\dot{C}_{B26} - \dot{C}_{B25}$	$c_{B26} = c_{B25}$ $c_{B17} = c_{B18}$
R-201	$\dot{C}_{B6} + \dot{C}_{B2} - \dot{C}_{B7} - \dot{C}_{B9}$	$\dot{C}_{B10}$	$c_{B7} = c_{B6}$ $c_{B9} = c_{B6}$
R-202	$(\dot{C}_{B13} - \dot{C}_{B14}) + (\dot{C}_{B23} - \dot{C}_{B24}) + \dot{C}_{B10}$	$\dot{C}_{B15}$	$c_{B23} = c_{B24}$ $c_{B14} = c_{B13}$
Overall System	$\dot{C}_{heating} - \dot{C}_{cooling} + \dot{C}_{S6} - \dot{C}_{S8} + \dot{C}_{S1} + \dot{C}_{S15} + \dot{C}_{B5} - (\dot{C}_{B7} - \dot{C}_{B9}) + \dot{C}_{B13} - \dot{C}_{B14}$	$\dot{C}_{B16} + \dot{C}_{S16}$	

Table 4
Validation of the models.

Component	Parameter	This work	Literature	Absolute Error
D-101	Final moisture (%, wb)	12.4	12.4 [35]	0
S-101	Yield (%, db)	15.0	15.0 [41]	0
R-101	CO_2	0.370	0.373 [21]	0.003
	CO	0.100	0.040 [21]	0.060
	CH_4	0.430	0.526 [21]	0.096
	H_2	0.020	0.061 [21]	0.041
R-202	Yield	82.0	87.3 [40]	5.3
	Linoleic Acid	0.37	0.41 [40]	0.04
	Palmitic Acid	0.36	0.36 [40]	0.00
	Oleic	0.14	0.14 [40]	0.00
	Stearic	0.08	0.08 [40]	0.00

derivatives. Therefore, this production process is focused on using the chemical exergy of biomass through chemical reactions, for the transformation into biofuels.

Table 6 shows the exergy of the fuel ($\dot{E}_F$), the exergy of the product ($\dot{E}_P$), the exergy destruction ($\dot{E}_D$) and the exergetic efficiency (η) for each component and for the overall system. The components E−201, E−202 and E−203 have an exergy destruction rate lower than 0.5 kW, therefore they were excluded from the table. It can be observed that the E−101 and D-101 are the main sources of irreversibility, they cause 53% and 28% of the overall exergy destruction rate, respectively. Similar results were found in a spray drying process of instant coffee [53] where the dryer was responsible for 23% of the exergy destruction. Similarly, Mehrpooya et al. [12] reported that air heat exchangers based on steam were the components with the lowest exergetic efficiency in the drying process of wood chips because a great amount of high quality energy was destroyed when the air was discharged.

Some studies show that the heat source in heat exchangers significantly affects the exergy destruction rate. When the heat source is flue gases, the exergy destruction rate is reduced [55]. Singh et al. [56] found that the use of solar energy for heating air increased the exergetic efficiency of the heat exchanger and the dryer from 15.3% to 24%. Another reason for a low exergetic efficiency is the high drying temperature. Beigi et al. [57] identified that an increase in the air temperature, increases the rate of heat and mass transfer and thus, increases the exergy of the exhaust air and the exergy losses.

Additionally, other components such as the R-202 and the R-101 destroy 5% of the overall destroyed exergy. Ofori-Boateng et al. [58] identified that transesterification reactors have a high exergy destruction rate because the reaction produces glycerin as a by-product and it has a high chemical exergy. Some factors that reduced the exergetic efficiency of these reactors were a high concentration of the catalyst, a high methanol/oil ratio and a high temperature of reaction [59]. Regarding the gasifier, Ji-chao et al. [60] found that unwanted products in the reaction such as char, increase the exergy destruction rate of this component, because it has a high

Table 5
Thermodynamic values of the streams.

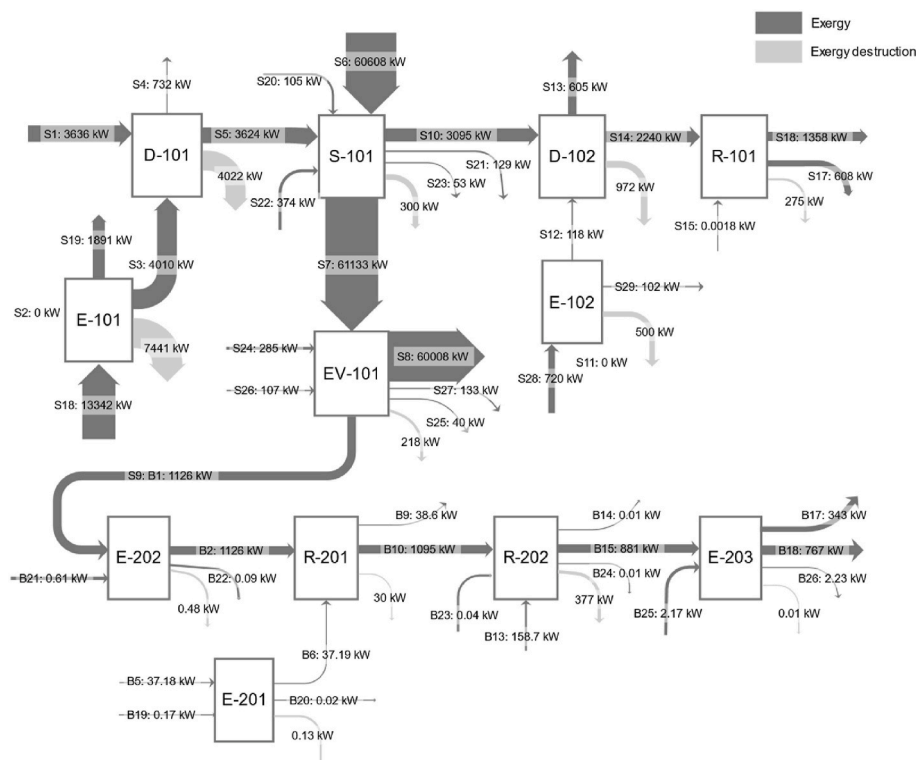| State	$\dot{m}$ (kg/h)	T (°C)	P (bar)	h (kJ/kg)	s (kJ/kg K)	$\dot{E}^{ph}$ (kW)	$\dot{E}^{ch}$ (kW)	$\dot{E}$ (kW)
S1	1071	30	1	197	0.5905	6.2	3630	3636
S2	562,075	25	1	0	0.0000	0.0	0	0
S3	562,075	150	1	151	0.4206	4010.0	0	4010
S4	562,670	80	1	57	0.1763	730.3	2	732
S5	476	80	1	159	0.4873	1.9	3622	3624
S6	4570	25	1	0	0.0000	0.0	60,608	60,608
S7	4586	68	1	71	0.2238	6.0	61,127	61,133
S8	4524	69	1	72	0.2264	6.1	60,001	60,008
S9	62.5	30	1	11	0.0350	0.0	1126	1126
S10	459	68	1	113	0.3517	1.0	3094	3095
S11	50,651	25	1	0	0.0000	0.0	0	0
S12	50,651	100	1	78	0.2330	118.0	0	118
S13	50,746	60	1	36	0.1156	27.4	578	605
S14	365	60	1	94	0.2967	0.6	2240	2240
S15	0.01	25	1	0	0.0000	0.0	0	0
S16	289	425	1	876	1.9150	24.5	1334	1358
S17	75.8	900	1	981	1.5350	11.4	596	608
S18	34,874	190	13	2681	6.1420	8234.0	5108	13,342
S19	34,874	190	13	702	1.8670	1408.0	484	1891
S20	7550	25	1	0	0.0000	0.0	105	105
S21	7550	68	1	179	0.5596	24.5	105	129
S22	976	190	13	2681	6.1420	230.5	143	374
S23	976	190	13	702	1.8670	39.4	14	53
S24	745	190	13	2681	6.1420	175.8	109	285
S25	745	190	13	702	1.8670	30.1	10	40
S26	7680	25	1	0	0.0000	0.0	107	107
S27	7680	69	1	184	0.5750	26.3	107	133
S28	1882	190	13	2681	6.1420	444.3	276	720
S29	1882	190	13	702	1.8670	76.0	26	102
B1	63	30	1	11	0.0350	0.0	1126	1126
B2	63	54	1	61	0.1959	0.1	1126	1126
B3	6	30	1	12	0.0391	0.0	2	1909
B4	6	30	1	13	0.0424	0.0	39	39
B5	12	25	1	0	0.0000	0.0	37	37
B6	12	54	1	72	0.2306	0.0	37	37
B7	1	54	1	61	0.1958	0.0	0	0
B8	71	54	1	64	0.2036	0.1	1125	1125
B9	11	54	1	93	0.2963	0.0	39	39
B10	63	53	1	57	0.1824	0.0	1095	1095
B11	26	30	1	13	0.0424	0.0	159	159
B12	1	30	1	17	0.0580	0.0	0	0
B13	26	30	1	13	0.0428	0.0	159	159
B14	0	54	1	77	0.2464	0.0	0	0
B15	89	54	1	46	0.1471	0.1	881	881
B16	89	30	1	7826	0.0260	0.0	881	881
B17	34	30	1	11	0.0352	0.0	343	343
B18	55	30	1	6607	0.0220	0.0	767	767
B19	0	190	13	2681	6.1420	0.1	0	0
B20	0	190	13	703	1.8690	0.0	0	0
B21	2	190	13	2681	6.1420	0.4	0	1
B22	2	190	13	703	1.8690	0.1	0	0
B23	0	190	13	2681	6.1420	0.0	0	0
B24	0	190	13	703	1.8690	0.0	0	0
B25	156	27	1	8366	0.0280	0.0	2	2
B26	156	40	1	63	0.2053	0.1	2	2

chemical exergy. Another study identified that parameters such as a high initial humidity of the biomass [61] and a low gasifying agent/biomass mass ratio [62] decreased the exergetic efficiency of the gasifier.

Furthermore, the components with the least impact on the overall exergy destruction rate are the E−201 and E−202, because they destroy less than 1%. Fig. 2 shows the exergy flows rates across the process. It can be observed that the S-101 and EV-101 have an input exergy rate higher than 60 MW. This occurs because the input solvent has the highest chemical exergy rate. That is why the recuperation of the solvent in the EV-101 is so important in order to reduce the exergy destruction rate and the operating costs. A previous experimental study showed that the use of a recycled solvent in the extraction process did not affect the extraction yield of SCG oil [63].

Table 6
Results of the exergetic analysis of all the main components of the process.

Component	$\dot{E}_F$ (kW)	$\dot{E}_P$ (kW)	$\dot{E}_D$ (kW)	η (%)	y^*_D	y_D
E−101	11,451	4010	7441	35	0.526	0.050
D-101	7646	3624	4022	47	0.285	0.027
S-101	61,433	61,133	300	99	0.021	0.002
EV-101	61,351	61,133	217	99	0.015	0.001
E−102	617	118	499	19	0.035	0.003
D-102	3213	2240	972	69	0.069	0.006
R-101	1633	1358	274	83	0.019	0.002
R-201	1125	1095	30	97	0.000	0.000
R-202	1254	877	376	70	0.000	0.000
Overall System	149,725	135,588	14,135	91	1.000	1.000

Fig. 2. Grassmann's diagram of the process.

Table 7
Results of exergoeconomic analysis.

Component	PEC ($)	c_f ($/MJ)	$\dot{Z}_k^{CI}$ ($/h)	$\dot{Z}_k^{O\&M}$ ($/h)	$\dot{Z}_k + \dot{C}_D$($/h)	$\dot{C}_D$ ($/h)	f_k	r_k
E−101	1415	0.028	0.44	0.25	759.20	758.50	0.09	1.86
D-101	6000	0.042	1.87	1.08	617.40	614.40	0.48	1.12
S-101	15,000	0.005	4.69	2.69	12.94	5.56	57.02	0.01
EV-101	5000	0.006	1.56	0.90	7.06	4.60	34.85	0.01
E−102	1415	0.028	0.44	0.25	51.65	50.96	1.35	4.29
D-102	6000	0.011	1.87	1.08	41.73	38.78	7.07	0.47
R-101	10,000	0.015	3.12	1.79	19.95	15.03	24.66	0.27
E−201	3000	0.028	0.82	0.42	1.25	0.01	98.93	1121.00
E−202	3000	0.028	0.82	0.42	1.29	0.05	96.22	269.00
R-201	25,000	0.001	6.80	3.49	10.44	0.14	98.67	2.10
R-202	20,000	0.003	5.44	2.79	12.90	4.66	63.87	1.20
E−203	4000	0.014	1.09	0.56	1.65	0.00	99.96	628.00

3.3. Exergoeconomic analysis

The total investment cost for the plant of syngas and biodiesel from SCG is estimated to be $13.2 million. The annual fuel cost and the operation and maintenance costs are $375,100 and $49,820 dollars, respectively, for a production of 289 kg/h of syngas and 55 kg/h of biodiesel, from processing a mass flow of 41,500 kg/h of SCG.

Table 7 shows the purchase equipment cost (*PEC*), the specific fuel costs (c_f), the capital investment cost rate ($\dot{Z}_k^{CI}$), the operational and maintenance cost rate ($\dot{Z}_k^{O\&M}$), the total operational cost rates ($\dot{Z}_k + \dot{C}_D$), the exergy destruction cost rate ($\dot{C}_D$), the exergoeconomic factor (f_k), and the relative difference (r_k) for each component. It can be observed that the components with the highest purchased costs such as R-201 and R-202 are not the components with the highest operational cost rates. Also there are other components with lower investment costs that have higher exergy destruction cost rates, such as the heat exchangers and the dryers.

Fig. 3 shows that the E−101 and the D-101 are the components with the highest operating costs rates ($\dot{Z}_k + \dot{C}_D$), followed by the E−102 and the D-102. This means that the air heater and the dryer influence significantly the overall costs of the system. These components have an exergoeconomic factor (f_k) of less than 10%, which means that the predominant cost is related to the destruction of exergy. At the same time, these components have the highest exergy destruction rate. Similar results have been found in a study related to a food drying process [64], where the dryer and the air heat exchanger presented an exergoeconomic factor of less than 5%.

A previous study had demonstrated that the avoidable exergy destruction cost rate could be more than 50% in components such as dryers or heat exchangers. Therefore, if the exergy destruction cost rate is reduced by at least 50% in D-101 and E−101, the overall operational cost of the process can be reduced by 45% and the overall exergetic efficiency could increase from 90.6% to 94.4%.

In order to reduce costs, it is possible to optimize the operational conditions of the process and to analyze the different factors that significantly affect the exergy destruction cost rate. A previous study [65] proposed solar heat pump dryers, which allowed the reduction of the exergy destruction cost rate from $0.06/h to $0.0044/h and the increase in the f_k from 5% to 51%; so that a balance is reached between the investment cost and exergy destruction cost rate with this structural change. Another study identified that recycling the drying air in continuous dryers has an economic and exergetic benefit for the process [66]. S. Zohrabi et al. [67] studied the recirculation of air in a convective dryer and achieved an increase of the exergetic efficiency from 55% to 95%.

According to different studies, the gasifier is one of the components that has the highest exergy destruction cost rate. Fakhim-ghanbarzadeh et al. [68] determined that this component was responsible for 11% of the operational cost rate and that it could be reduced 10% by increasing the temperature of the reaction and reducing the biomass/gasifying agent mass ratio. Fani et al. [69] found that the decrease of pressure in the reactor also reduces the cost rate. In addition, there are other important factors that are more dependent on the fuel used to operate the plant's facilities [70]. In a previous study, the specific cost of the gasifying agent was found to be key in this cost rate [71].

The dead state temperature is also another important factor because it is determined by the initial condition of the air and the water used in the system and influences the exergy rates of each process stream. This variable changes over time, as it depends on climatic changes. Fig. 4 shows the effect of the dead state temperatures between 15 °C and 35 °C on the exergy destruction rate and the cost of exergy destruction rate. The results are favorable for high dead state temperatures, and a 10°C change reduces the process cost rate by $150/h.

Fig. 5 shows the components of the process that are most affected by the change of the dead state temperature; in this case, they are the components with the highest exergy destruction cost rate. This means that the overall operational cost rate could be reduced by $300/h when the temperature of the environment is increased. Erbay et al. [72] presented similar results when they analyzed the effect of the dead state temperature between 0 and 20 °C in the exergetic efficiency and total exergy costs of a ground-source heat pump food dryer. Other components such as the R-101 are not significantly affected by the change of the dead state temperature, because they do not have inputs from the environment. Dryers and heat exchangers require ambient air, which means that environmental conditions strongly affect the performance of these components.

4. Conclusions

The integrated production process of biodiesel and syngas from spent coffee grounds was simulated and evaluated by an exergoeconomic analysis. The model was validated with experimental data obtaining a maximum relative error of 6%. The exergetic and economic indicators were determined at a component level and an overall system level.

The economic analysis revealed that the first stage of the process, which includes the pretreatment of the biomass and the oil extraction, has a lower capital investment cost rate but a higher operating and maintenance cost rate than the stage of syngas and biodiesel production.

The overall exergetic efficiency of the process was 91% with an exergy destruction rate of 14,135 kJ/s. The overall exergy destruction cost rate ($1,493/h) represents 97% of the total cost rate of the plant. The main components that caused the highest exergy destruction rates and cost rates were the SGC dryers (D-101 and D-201) and the air heat exchangers (E−101 and E−201). These components are responsible for 92% of the overall exergy destruction cost rate.

An increase in the dead state temperature could reduce the exergy destruction cost rate of the process up to 9%. The biodiesel and syngas specific costs could be reduced by maximizing the exergetic efficiency and minimizing the exergy destruction rate in the dryers and the air heat exchangers.

An advanced exergoeconomic analysis should be performed in order to quantify the avoidable exergy destruction cost rate, mainly in the dryers and air heat exchangers.
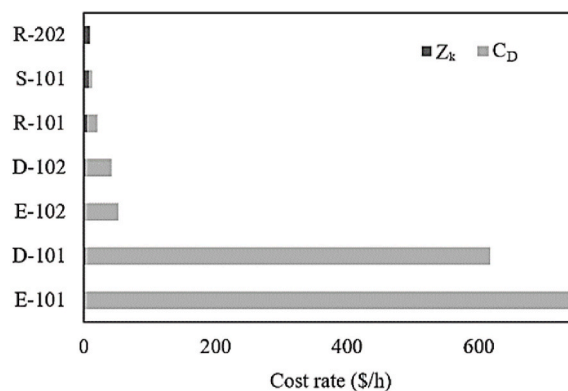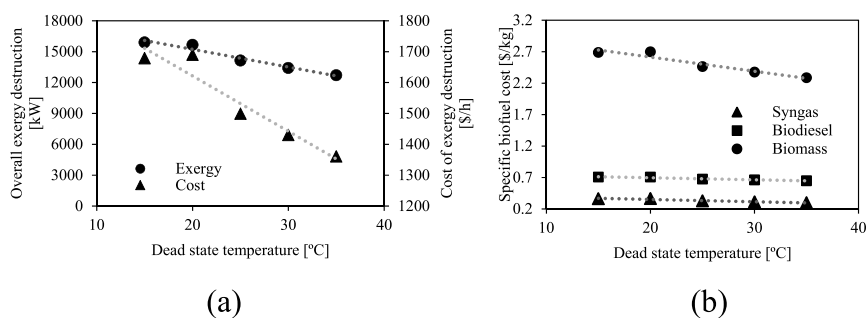
Fig. 3. Main operational cost rates.

(a)   (b)

Fig. 4. Effect of dead state temperature on a) overall exergy destruction and cost of exergy destruction and b) specific biofuels cost.
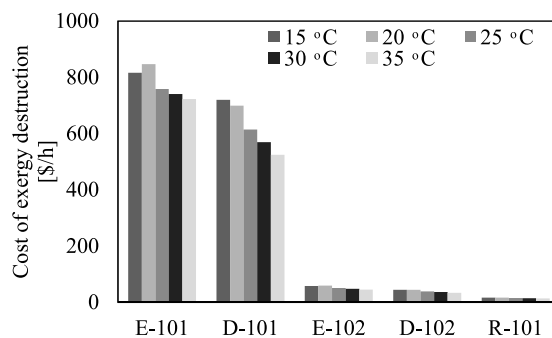

Fig. 5. Effect of the dead state temperature on the costs of exergy destruction of the main components.

Finally, it can be concluded that the exergetic and economic analyses reveal the components that are responsible for the highest exergy destruction rate and also the components that have a greater impact on the final product cost of the process. In order to increase the feasibility and sustainability of the process, future research should be focused on integrating different sources of energy, including renewable sources, for the air heating in order to minimize the exergy destruction rate in the drying process. Furthermore, experimental analysis are considered necessary to determine the impact of operational parameters and structural changes on the SCG drying process.

Informed consent

Informed consent has been obtained from all individuals included in this study.

CRediT authorship contribution statement

Diana L. Tinoco-Caicedo: Conceptualization, Investigation, Data curation, Writing – original draft. **Medelyne Mero-Benavides:** Software, Validation, Formal analysis, Writing – original draft. **Myrian Santos-Torres:** Software, Validation, Formal analysis, Writing – original draft. **Alexis Lozano-Medina:** Supervision, Project administration. **Ana M. Blanco-Marigorta:** Methodology, Writing – review & editing, Supervision, Project administration.

Declaration of Competing Interest

The authors declare that they have no known competing financial interests or personal relationships that could have appeared to influence the work reported in this paper.

Acknowledgements

Nomenclature

c	unit exergy cost ($/MJ)
c_p	heat capacity (kJ/kg K)
$\dot{C}$	cost rate associated with an exergy stream ($/h)
e	specific exergy rate (kJ/kg)
$\dot{E}$	exergy rate (kJ/h)
f	exergoeconomic factor
h	specific enthalpy (kJ/kg)
$\overline{HHV}$	High heating value (MJ/kg)
$\dot{m}$	mass flow rate (kg/h)
n	lifetime of the system (years)
P	pressure (kPa)
r	relative cost difference
R	ideal gas constant (kJ/kmol K)
s	specific entropy (kJ/kg)
T	temperature (°C)
w	mole fraction of water vapor
x	mole fraction
y	destruction rate
y*	relative irreversibility
$\dot{Z}$	investment cost rate ($/h)

Greek letters

Δ	difference
η	exergetic efficiency (%)

Superscript

ch	chemical
ph	physical

Subscripts

B	biodiesel process
CI	cost investment
D	destruction
DB	dry biomass
F	fuel
gly	glycerin compound
i	ith compound
k	kth component
L	loss
o	thermodynamic environment
O&M	operation and maintenance
P	product

R   Reagents
S   oil extraction and syngas process
x   hydrocarbon fuels
WB   wet biomass

Abbreviations

D   dryer
E   heat exchanger
EV   evaporator
FFA   free fatty acids
NIST   National Institute of Standards and Technology
O&M   operation and maintenance
PEC   purchased equipment cost
PFI   Plant-facilities investment
R   Reactor
S   soxhlet
SC   spent coffee
SCG   spent coffee ground
TDE   ThermoData Engine
UNIQUAC   Universal quasichemical

References

[1] M.K. Yesilyurt, C. Cesur, V. Aslan, Z. Yilbasi, The production of biodiesel from safflower (Carthamus tinctorius L.) oil as a potential feedstock and its usage in compression ignition engine: a comprehensive review, Renew. Sustain. Energy Rev. 119 (2020) 109574.

[2] F. Martins, C. Felgueiras, M. Smitkova, N. Caetano, Analysis of fossil fuel energy consumption and environmental impacts in european countries, Energies 12 (2019) 1–11.

[3] M.A. Mayorga, J.G. Cadavid Estrada, J.A. Bonilla Paez, C. Lopez, M. Lopez, Se of biofuels in the aeronautical industry. Case of the Colombian air force, Tecciencia 14 (2019) 33–43.

[4] D. Zhu, S.M. Mortazavi, A. Maleki, A. Aslani, H. Yousefi, Analysis of the robustness of energy supply in Japan: role of renewable energy, Energy Reports 6 (2020) 378–391.

[5] C.H.W. Ruhe, Statistical review, JAMA, J. Am. Med. Assoc. 225 (2019) 299–306.

[6] S.S. Hassan, G.A. Williams, A.K. Jaiswal, Lignocellulosic biorefineries in Europe: current state and prospects, Trends Biotechnol. 37 (2019) 231–234.

[7] S. Datta, Arup; Hossain, Aslam; Roy, an overview on biofuels and their advantages and disadvantages, Asian J. Chem. 26 (2014) 70–73.

[8] A.B. Guerrero, E. Muñoz, Life cycle assessment of second generation ethanol derived from banana agricultural waste: environmental impacts and energy balance, J. Clean. Prod. 174 (2018) 710–717.

[9] M.A. Rajaeifar, A. Akram, B. Ghobadian, S. Rafiee, R. Heijungs, M. Tabatabaei, Environmental impact assessment of olive pomace oil biodiesel production and consumption: a comparative lifecycle assessment, Energy 106 (2016) 87–102.

[10] J.H. Ebner, R.A. Labatut, J.S. Lodge, A.A. Williamson, T.A. Trabold, Anaerobic co-digestion of commercial food waste and dairy manure: characterizing biochemical parameters and synergistic effects, Waste Manag. 52 (2016) 286–294.

[11] D.Y.C. Leung, L.C. Yu, G.C.K. Lam, H.Y.H. Kwok, W.K. Cheng, Bioethanol: is it a suitable biofuel for Hong Kong for reducing its vehicular emissions and carbon footprint? Energy Procedia 142 (2017) 2892–2897.

[12] M. Mehrpooya, M. Khalili, M.M.M. Sharifzadeh, Model development and energy and exergy analysis of the biomass gasification process (Based on the various biomass sources), Renew. Sustain. Energy Rev. 91 (2018) 869–887.

[13] L. Pattanaik, F. Pattnaik, D.K. Saxena, S.N. Naik, Biofuels from Agricultural Wastes, Elsevier Inc., 2019.

[14] K.K. Jaiswal, B. Jha, R.A. Prasath, Biodiesel production from discarded fish waste for sustainable clean energy development, J. Chem. Pharm. Sci. 2014-Decem (2014) 113–114.

[15] J.J. Milledge, The challenge of algal fuel : economic processing of the entire algal biomass, Condens. Matter -Materials Eng. Newsl. (2010) 1–5.

[16] R.W. Jenkins, N.E. Stageman, C.M. Fortune, C.J. Chuck, Effect of the type of bean, processing, and geographical location on the biodiesel produced from waste coffee grounds, Energy Fuel. 28 (2014) 1166–1174.

[17] Y. Liu, Q. Tu, G. Knothe, M. Lu, Direct transesterification of spent coffee grounds for biodiesel production, Fuel 199 (2017) 157–161.

[18] M.J. Haas, K. Wagner, Simplifying biodiesel production: the direct or in situ transesterification of algal biomass, Eur. J. Lipid Sci. Technol. 113 (2011) 1219–1229.

[19] J. Park, B. Kim, J.W. Lee, In-situ transesterification of wet spent coffee grounds for sustainable biodiesel production, Bioresour. Technol. 221 (2016) 55–60.

[20] T.R. Pacioni, D. Soares, M. Di Domenico, M.F. Rosa, R.D.F.P.M. Moreira, H.J. José, Bio-syngas production from agro-industrial biomass residues by steam gasification, Waste Manag. 58 (2016) 221–229.

[21] H.A. Kibret, Y.-L. Kuo, T.-Y. Ke, Y.-H. Tseng, Gasification of Spent Coffee Grounds in a Semi-fluidized Bed Reactor Using Steam and CO 2 Gasification Medium, 2021, 000.

[22] Z.A. Antonova, V.S. Krouk, Y.E. Pilyuk, Y.V. Maksimuk, L.S. Karpushenkava, M.G. Krivova, Exergy analysis of canola-based biodiesel production in Belarus, Fuel Process. Technol. 138 (2015) 397–403.

[23] A. Amelio, T. Van De Voorde, C. Creemers, J. Degrève, S. Darvishmanesh, P. Luis, B. Van Der Bruggen, Comparison between exergy and energy analysis for biodiesel production, Energy 98 (2016) 135–145.

[24] R.A.M. Boloy, M.E. Silva, A.E. Valle, J.L. Silveira, C.E. Tuna, Thermoeconomic analysis of hydrogen incorporation in a biodiesel plant, Appl. Therm. Eng. 113 (2017) 519–528.

[25] E. Shayan, V. Zare, I. Mirzaee, On the use of different gasification agents in a biomass fueled SOFC by integrated gasifier: a comparative exergo-economic evaluation and optimization, Energy 171 (2019) 1126–1138.

[26] Y. Wu, W. Yang, W. Blasiak, Energy and exergy analysis of high temperature agent gasification of biomass, Energies 7 (2014) 2107–2122.

[27] H. Ansarinasab, M. Mehrpooya, M. Sadeghzadeh, Life-cycle assessment (LCA) and techno-economic analysis of a biomass-based biorefinery, J. Therm. Anal. Calorim. 145 (2021) 1053–1073.

[28] T. Nakyai, Y. Patcharavorachot, A. Arpornwichanop, D. Saebea, Comparative exergoeconomic analysis of indirect and direct bio-dimethyl ether syntheses based on air-steam biomass gasification with CO2 utilization, Energy 209 (2020) 118332.

[29] M. Aghbashlo, M. Tabatabaei, S. Soltanian, H. Ghanavati, A. Dadak, Comprehensive exergoeconomic analysis of a municipal solid waste digestion plant equipped with a biogas genset, Waste Manag. 87 (2019) 485–498.

[30] I. Polygeneration, P. Plant, B.S.S. Firing, M. Alghassab, O.D. Samuel, Z.A. Khan, M. Imran, M. Farooq, Exergoeconomic and Environmental Modeling of, 2020.

[31] T. Murakami, G. Xu, T. Suda, Y. Matsuzawa, H. Tani, T. Fujimori, Some process fundamentals of biomass gasification in dual fluidized bed, Fuel 86 (2007) 244–255.

[32] D.R. Vardon, B.R. Moser, W. Zheng, K. Witkin, R.L. Evangelista, T.J. Strathmann, K. Rajagopalan, B.K. Sharma, Complete utilization of spent coffee grounds to produce biodiesel, bio-oil, and biochar, ACS Sustain. Chem. Eng. 1 (2013) 1286–1294.

[33] C.H. Dang, T.D. Nguyen, Physicochemical characterization of Robusta spent coffee ground oil for biodiesel manufacturing, Waste and Biomass Valorization 10 (2019) 2703–2712.

[34] J.L. Díaz de Tuesta, A. Quintanilla, D. Moreno, V.R. Ferro, J.A. Casas, Simulation and optimization of the CWPO process by combination of aspen plus and 6-factor doehlert matrix: towards autothermal operation, Catalysts 10 (2020).

[35] F.J. Gómez-de la Cruz, J.M. Palomar-Carnicero, Q. Hernández-Escobedo, F. Cruz-Peragón, Experimental studies on mass transfer during convective drying of spent coffee grounds generated in the soluble coffee industry, J. Therm. Anal. Calorim. 145 (2021) 97–107.

[36] E.C. Carlson, Don't gamble with physical properties for simulations - aspen Technology, Inc., Chem. Eng. Prog. (1996) 35–46.

[37] J. Han, Y. Liang, J. Hu, L. Qin, J. Street, Y. Lu, F. Yu, Modeling downdraft biomass gasification process by restricting chemical reaction equilibrium with Aspen Plus, Energy Convers. Manag. 153 (2017) 641–648.

[38] L.P.R. Pala, Q. Wang, G. Kolb, V. Hessel, Steam gasification of biomass with subsequent syngas adjustment using shift reaction for syngas production: an Aspen Plus model, Renew. Energy 101 (2017) 484–492.

[39] D. Han, X. Yang, R. Li, Y. Wu, Environmental impact comparison of typical and resource-efficient biomass fast pyrolysis systems based on LCA and Aspen Plus simulation, J. Clean. Prod. 231 (2019) 254–267.

[40] M. Haile, Integrated volarization of spent coffee grounds to biofuels, Biofuel Res. J. 1 (2014) 65–69.

[41] M.M.R. De Melo, H.M.A. Barbosa, C.P. Passos, C.M. Silva, Supercritical fluid extraction of spent coffee grounds: measurement of extraction curves, oil characterization and economic analysis, J. Supercrit. Fluids 86 (2014) 150–159.

[42] O.O.D. Afolabi, M. Sohail, Y.L. Cheng, Optimisation and characterisation of hydrochar production from spent coffee grounds by hydrothermal carbonisation, Renew. Energy 147 (2020) 1380–1391.

[43] A.B.A. de Azevedo, T.G. Kieckbush, A.K. Tashima, R.S. Mohamed, P. Mazzafera, S.A.B.V. de Melo, Extraction of green coffee oil using supercritical carbon dioxide, J. Supercrit. Fluids 44 (2008) 186–192.

[44] B. Leśniak, L. Słupik, G. Jakubina, The determination of the specific heat capacity of coal based on literature data, Chemik 67 (2013) 560–571.

[45] C. Dupont, R. Chiriac, G. Gauthier, F. Toche, Heat capacity measurements of various biomass types and pyrolysis residues, Fuel 115 (2014) 644–651.

[46] D.A. Jahn, F.O. Akinkunmi, N. Giovambattista, Effects of temperature on the properties of glycerol: a computer simulation study of five different force fields, J. Phys. Chem. B 118 (2014) 11284–11294.

[47] D.R. Morris, J. Szargut, Standard chemical exergy of some elements and compounds on the planet earth, Energy 11 (1986) 733–755.

[48] W.J. Wepfer, R. Gagglio, E.F. Obert, in: Proper Evaluation of Available Energy for HVACe, ASHRAE Trans., 1979, pp. 214–230.

[49] A. Bejan, G. Tsatsaronis, M. Moran, Thermal Design & Optimization, John Wiley & Sons, Inc., Canada, 1996.

[50] G. Song, L. Shen, J. Xiao, L. Chen, Estimation of specific enthalpy and exergy of biomass and coal ash, Energy Sources, Part A Recover, Util. Environ. Eff. 35 (2013) 809–816.

[51] S.V. Vassilev, D. Baxter, L.K. Andersen, C.G. Vassileva, An overview of the chemical composition of biomass, Fuel 89 (2010) 913–933.

[52] ASTM International, Standard Test Method for Heat of Combustion of Liquid Hydrocarbon Fuels by Bomb Calorimeter (Reapproved 2007), ASTM Stand. D240-02. i, 2009, pp. 1–9.

[53] D.L. Tinoco-Caicedo, A. Lozano-Medina, A.M. Blanco-Marigorta, Conventional and advanced exergy and exergoeconomic analysis of a spray drying system: a case study of an instant coffee factory in Ecuador, Energies 13 (2020).

[54] Interagua, Informe Anual 2018-2019, Guayaquil, 2019.

[55] H. Sheikhshoaei, M. Dowlati, M. Aghbashlo, M.A. Rosen, Exergy analysis of a pistachio roasting system, Dry. Technol. 38 (2020) 1565–1583.

[56] A. Singh, J. Sarkar, R.R. Sahoo, Experimental energy, exergy, economic and exergoeconomic analyses of batch-type solar-assisted heat pump dryer, Renew. Energy 156 (2020) 1107–1116.

[57] M. Beigi, M. Tohidi, M. Torki-Harchegani, Exergetic Analysis of Deep-Bed Drying of Rough Rice in a Convective Dryer, 2017.

[58] C. Ofori-Boateng, T.L. Keat, L. Jitkang, Feasibility study of microalgal and jatropha biodiesel production plants: exergy analysis approach, Appl. Therm. Eng. 36 (2012) 141–151.

[59] K. Khoobbakht, K. Kheiralipour, H. Rasouli, M. Rafiee, M. Hadipour, M. Karimi, Experimental exergy analysis of transesterification in biodiesel production, Energy 196 (2020).

[60] Y. Ji-chao, B. Sobhani, Integration of biomass gasification with a supercritical CO2 and Kalina cycles in a combined heating and power system: a thermodynamic and exergoeconomic analysis, Energy 222 (2021) 119980.

[61] M. Hosseini, I. Dincer, M.A. Rosen, Steam and air fed biomass gasification: comparisons based on energy and exergy, Int. J. Hydrogen Energy 37 (2012) 16446–16452.

[62] D. Tapasvi, R.S. Kempegowda, K.Q. Tran, Ø. Skreiberg, M. Grønli, A simulation study on the torrefied biomass gasification, Energy Convers. Manag. 90 (2015) 446–457.

[63] L. Jin, H. Zhang, Z. Ma, Study on capacity of coffee grounds to be extracted oil, produce biodiesel and combust, Energy Procedia 152 (2018) 1296–1301.

[64] Z. Erbay, A. Hepbasli, Assessment of cost sources and improvement potentials of a ground-source heat pump food drying system through advanced exergoeconomic analysis method, Energy 127 (2017) 502–515.

[65] H. Atalay, Comparative Assessment of Solar and Heat Pump Dryers with Regards to Exergy and Exergoeconomic Performance, 2019.

[66] R.B. Keey, Introduction to Industrial Drying Operation, Pergamon Press, New York, 1978.

[67] S. Zohrabi, S.S. Seiiedlou, M. Aghbashlo, H. Scaar, J. Mellmann, Enhancing the exergetic performance of a pilot-scale convective dryer by exhaust air recirculation, Dry. Technol. 38 (2020) 518–533.

[68] B. Fakhimghanbarzadeh, B. Farhanieh, H. Marzi, A. Javadzadegan, Evolutionary algorithm for multi-objective exergoeconomic optimization of biomass waste gasification combined heat and power system, IEEE Int. Conf. Ind. Informatics (2009) 361–366.

[69] M. Fani, B. Farhanieh, A.A. Mozafari, Exergoeconomic optimization of black liquor gasification combined cycle using evolutionary and conventional iterative method, Int. J. Chem. React. Eng. 8 (2010).

[70] A. Abuadala, I. Dincer, Exergoeconomic analysis of a hybrid steam biomass gasification-based Tri-generation system, Prog. Exergy, Energy, Environ. (2014) 51–67.

[71] Y. Kalinci, A. Hepbasli, I. Dincer, Exergoeconomic analysis and performance assessment of hydrogen and power production using different gasification systems, Fuel 102 (2012) 187–198.

[72] Z. Erbay, A. Hepbasli, Exergoeconomic evaluation of a ground-source heat pump food dryer at varying dead state temperatures, J. Clean. Prod. 142 (2017) 1425–1435.